

04,15

# Acoustic properties of crystals with oxyborate structure $YAl_3(BO_3)_4$ and $HoAl_3(BO_3)_4$

© P.P. Turchin<sup>1,2</sup>, S.I. Burkov<sup>1</sup>, V.I. Turchin<sup>1</sup>, O.N. Pletnev<sup>1</sup>, M.Yu. Chulkova<sup>1</sup>

<sup>1</sup> Siberian Federal University,  
Krasnoyarsk, Russia

<sup>2</sup> Kirensky Institute of Physics, Federal Research Center KSC SB, Russian Academy of Sciences,  
Krasnoyarsk, Russia

E-mail: pturchin@sfu-kras.ru

Received July 1, 2024

Revised July 2, 2024

Accepted July 3, 2024

The anisotropy of the electromechanical parameters of acoustic waves (bulk, surface and SH waves, as well as Lamb waves) in yttrium and holmium aluminum borates, which are representatives of the single crystals family  $RM_3(BO_3)_4$  (where  $R = Y, La-Lu$ ;  $M = Fe, Al, Cr, Ga, Sc$ ) with unique properties of magnetoelectrics and multiferroics with a magnetic ion in the structure has been studied. The analysis of acoustic wave parameters is based on experimentally measured electromechanical constants  $C_{ijkl}$ ,  $e_{ijk}$ ,  $d_{ijk}$  and  $\epsilon_{ij}$ .

**Keywords:** crystals with the structure of oxyborates, acoustic bulk waves, surface waves, Lamb waves.

DOI: 10.61011/PSS.2024.09.59215.174

## 1. Introduction

Single-crystals of family of trigonal rare-earth oxyborates  $RM_3(BO_3)_4$  (where  $R = Y, La-Lu$ ;  $M = Fe, Al, Cr, Ga, Sc$ ) depending on composition and thermodynamic conditions have piezoelectric, magnetoelectric properties and properties of multiferroics [1–3]. In ferrobates ( $RFe_3(BO_3)_4$ ) giant magnetoelectric [4] and magnetodielectric [5] effects are determined, aluminoborates  $RA_3(BO_3)_4$  are have potential for use in laser engineering [6–9]. Most recently interest increases to study the physical properties of these crystals, first of all, to study microscopic magnetic-elastic-electric interactions in them, but also to extend their application in functional electronics [4,5,10–15].

Yttrium aluminoborate  $YAl_3(BO_3)_4$  (YBO) and holmium aluminoborate  $HoAl_3(BO_3)_4$  (HBO) (point symmetry 32) in series of oxyborates are nonmagnetic and magnetoelectric single-crystals, respectively, and can characterise the anisotropy of elastic-electric and magnetoelectric interaction in them. Previously by echo-pulse ultrasound [16] and quasistatic [16,17] methods we obtained the experimental values of electromechanical constants of YBO single-crystal at room temperature. In present paper similar studies are made for HBO single-crystals. The experimental values of material constants of these single-crystals are used for comparative analysis of characteristics of bulk-acoustic-waves (BAW), surface acoustic waves (SAW), and dispersion of electromechanical characteristics of SH-waves and Lamb waves. Additionally effect of mass load pf metal layer on value of the electromechanical interaction in yttrium and holmium aluminoborates is studied, this effect accounting is necessary to design the ecoustic electronics devices.

## 2. Theory of elastic waves propagation and determination of material constants of crystal

For small-amplitude waves in piezoelectric crystal the wave equation, the equations of electrostatics, and the equations of state of the piezoelectric medium have the form [18]:

$$\begin{aligned} \rho_0 \ddot{U}_i &= \tau_{ik,k}, & D_{m,m} &= 0. \\ \tau_{ik} &= C_{ikpq} \eta_{pq} - e_{nik} E_n, \\ D_n &= e_{nik} \eta_{ik} + \epsilon_{nm} E_m, \end{aligned} \quad (1)$$

In equation (1) the following designations are accepted:  $\rho_0$  — crystal density,  $U_i$  — vector of elastic offsets,  $\eta_{ik}$  and  $\tau_{ik}$  — tensors of infinitely small mechanical deformations and stresses,  $E_i$  and  $D_i$  — vectors of stress and electric field, and induction,  $C_{ikpq}$ ,  $e_{nik}$  and  $\epsilon_{nm}$  — tensors of elastic, piezoelectric and dielectric constants. Hereafter the summation over a twice-repeated index is implied.

Propagation of acoustic waves in the piezoelectric wafer  $h$  thick shall correspond to boundary conditions [19,20], that mean equality to zero of components of tensor of normal stresses at interface crystal-vacuum. The continuity of the components of the electric field strength vector tangential to the interface is ensured by the condition of continuity of the electric potential  $\varphi$ , and by the continuity condition of normal components of induction vector [21].

See detail description of the method of experimental studies of values of elastic, piezoelectric and dielectric constants in paper [16]. The elastic constants were determined by the solution of inverse problem of the crystal acoustics [22] as per measured values of speeds of bulk

Values of electromechanical constants of single-crystals  $YAl_3(BO_3)_4$  and  $HoAl_3(BO_3)_4$ 

	Elastic constants $C_{\lambda\mu}, 10^{10} \text{ N/m}^2$						Dielectric constants $\varepsilon_{ij}/\varepsilon_0$	
	$C_{11}$	$C_{12}$	$C_{13}$	$C_{14}$	$C_{33}$	$C_{44}$		
YBO	$40.47 \pm 0.05$	$21.14 \pm 0.05$	$9.75 \pm 0.05$	$-2.35 \pm 0.1$	$27.09 \pm 0.05$	$7.49 \pm 0.01$	$9.67 \pm 0.05$	
HBO	$41.13 \pm 0.05$	$21.43 \pm 0.05$	$10.05 \pm 0.05$	$-2.1 \pm 0.1$	$27.33 \pm 0.05$	$7.57 \pm 0.01$	$9.85 \pm 0.05$	

	Piezoelectric constants $e_{i\lambda}, \text{ Q/m}^2, d_{i\lambda}, 10^{-12} \text{ Q/N}$				Dielectric constants $\varepsilon_{ij}/\varepsilon_0$	
	$e_{11}$	$e_{14}$	$d_{11}$	$d_{14}$		
YBO	$-1.06 \pm 0.07$	$-0.27 \pm 0.04$	$-6.0 \pm 0.3$	$-7.2 \pm 0.4$	$11.7 \pm 0.1$	$11.1 \pm 0.1$
HBO	$-1.02 \pm 0.07$	$-0.15 \pm 0.04$	$-6.1 \pm 0.3$	$-6.1 \pm 0.4$	$9.9 \pm 0.1$	$10.9 \pm 0.1$

acoustic waves (BAW) in base and turned crystallographic directions. To determine speeds of BAWs the ultrasound acoustic method of echo-pulse was used with accuracy of absolute measurements  $10^{-4}$ . Measurements were performed at frequency of 28 MHz. The absolute values of the piezoelectric constants were also determined by the measured values of speeds of BAWs, but for the piezoactive acoustic modes [16].

To clarify values of piezoelectric constants the quasistatic measurements of piezoelectric constants  $d_{ijk}$  were performed, the piezoelectric constant are linked with  $e_{ijk}$  by equation [23]:

$$e_{ijk} = d_{ilm} C_{lmjk}^E. \quad (2)$$

Under this method DMA 242 C device was used to create precision variable of dynamic load. Values of piezoelectric constants were determined by direct measurement of the piezoelectric effect in crystallophysical coordinate system, where  $C_{14} < 0$ . High-frequency dielectric permittivity was determined from values of low-frequency dielectric permittivity considering the piezoelectric contribution. Detail description of the measurement procedure of tensor modulus of elasticity, piezoelectric and dielectric constants in YBO crystal, performed earlier by authors, are described in papers [16,17].

Experimental data of linear electromechanical constants for single-crystals  $YAl_3(BO_3)_4$  and  $HoAl_3(BO_3)_4$  are given in Table.

### 3. Anisotropy of speeds and electromechanical coupling coefficient of acoustic waves in crystals $YAl_3(BO_3)_4$ and $HoAl_3(BO_3)_4$

Based on measured electromechanical constants of single-crystals  $YAl_3(BO_3)_4$  and  $HoAl_3(BO_3)_4$  (Table) the analysis of characteristics of acoustic wave propagation in these crystals was made.

The values of the phase speeds of BAWs, surface (SAW), Lamb waves, and SH waves were found by solving equations (1) taking into account the standard boundary

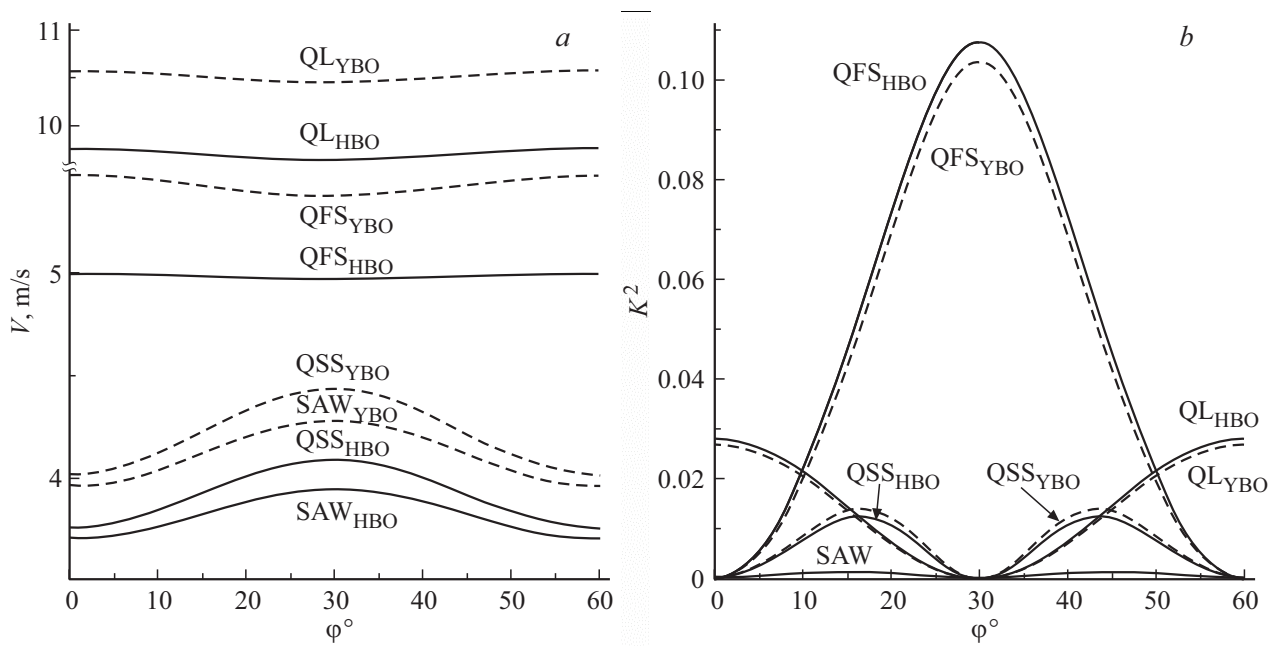
conditions and experimental values of the material constants given in the Table. Values of electromechanical coupling coefficient (EMCC)  $K^2$  for SAW, and Lamb waves were calculated by formula:

$$K^2 = 2 \frac{V - V_m}{V}, \quad (3)$$

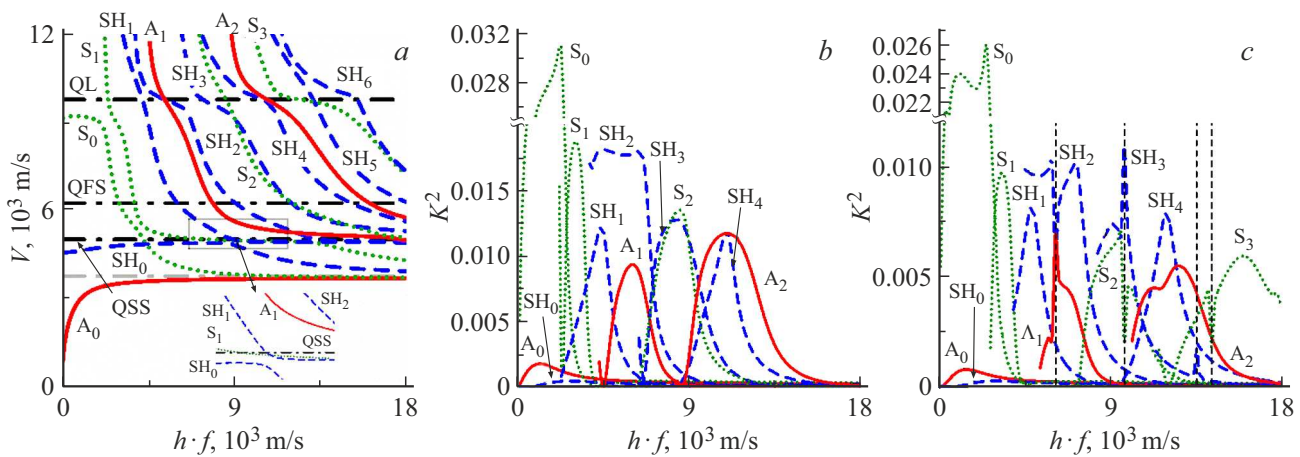
where  $V_m$  — phase speed on metallized surface.

Figure 1 presents anisotropy of parameters of BAW and SAW in plane (001) of single-crystals  $YAl_3(BO_3)_4$  and  $HoAl_3(BO_3)_4$ . In directions of elastic wave propagation in this plane the change in speeds of BAW of longitudinal (QL) and fast offset (QFS) waves is relatively low for both crystals. But these values significantly differ for different crystals. In particular, value of phase speed of QFS in direction [100] — 5479.8 m/s and 5004.3 m/s, but at angle  $30^\circ$  — 5384.6 m/s and 4980.4 m/s for crystals YBO and HBO, respectively (Figure 1, a). In plane (001) all BAWs are piezoactive. Maximum value of EMCC  $K^2$  is 0.103 and 0.107, and is reached in the direction at angle  $30^\circ$  with direction [100] for elastic wave QFS for crystals YBO and HBO, respectively (Figure 1, b). Note that although density of crystals YBO and HBO significantly differ, i.e.  $3720 \text{ kg/m}^3$  and  $4440 \text{ kg/m}^3$ , respectively, values of modulus of elasticity are rather close to each other (Table). So, insignificant differences are natural of absolute values of parameters at same anisotropy complying with point symmetry of crystals. Detail description of anisotropy of characteristics of BAW and SAW in single-crystal YBO is given in [16].

Figure 2 shows the dispersion dependences of phase speeds and  $K^2$  of Lamb waves and SH-wave in Z-cut in direction of elastic wave propagation [100] in crystal wafer HBO. Range of considered values  $h \times f$  (thickness  $\times$  frequency) is from 0 to 18000 m/s. Range of change of phase speeds of running Lamb waves and SH-waves — from value of phase speed of longitudinal QL BAW 9751.9 m/s to speed of SAW 3698 m/s in Z-cut. Maximum value of EMCC in wafer of crystal HBO with short-circuited one free surface for fundamental mode  $S_0$  of Lamb wave is reached in range  $h \times f$  from 250 m/s



**Figure 1.** Anisotropy of phase speeds and  $K^2$  BAW and SAW in Z-cut of crystals YBO and HBO. *a)* phase speeds; *b)*  $K^2$  — EMCC.



**Figure 2.** Dispersion dependences of phase speeds and EMCC  $K^2$  of Lamb wave and SH-wave in wafer of crystal HBO in direction of [100] Z-cut. *a)* phase speeds; *b)*  $K^2$  — metallization of both free surfaces; *c)*  $K^2$  — metallization of one free surface in plane (001).

to 3000 m/s and at  $h \times f = 2250$  m/s is  $K^2 = 0.02$  (Figure 2, *c*). But, in fundamental antisymmetric Lamb wave  $A_0$  and  $SH_0$  — mode EMCC values are lower by two orders of magnitude. Maximum EMCC value is  $K^2 = 0.0007$  at  $h \times f = 1350$  m/s and  $K^2 = 0.0002$  at  $h \times f = 2650$  m/s, respectively (Figure 2, *c*). In this case all modes of elastic wave are piezoelectric. EMCC values of modes of elastic waves of higher orders mainly are in range of 0.01 to zero when values  $h \times f$  increase. For wafer of crystal HBO with short circuited two free surfaces EMCC values are higher. In particular, for the fundamental modes  $S_0$ ,  $A_0$  and  $SH_0$  — mode EMCC values are 0.03, 0.028 and 0.005, respectively (Figure 2, *b*). Note, that for the crystal YBO behavior of characteristics of the elastic wave is

absolutely same, but EMCC values are higher by two times. In particular, maximum EMCC value for the fundamental mode  $S_0$  of Lamb wave in crystal YBO at  $h \times f = 2250$  m/s is  $K^2 = 0.04$ . Detail graph of dispersion dependences of La,b waves for the crystal YBO is given in [24].

Lamb waves propagation in the direction [100] of Z-cut is featured by presence of regions of interactions (hybridization) [25] between the Lamb wave modes, it occurs, mainly, in case of metallization of only one free surface of the crystalline wafer. In Figure 2, *c* points of modes interaction of elastic wave are marked by vertical dotted lines, in their region abrupt change occurs in EMCC values of interacting modes of elastic wave. For example, in the direction of [100] Z-cut between modes  $A_1$  and  $SH_2$  in range  $h \times f$

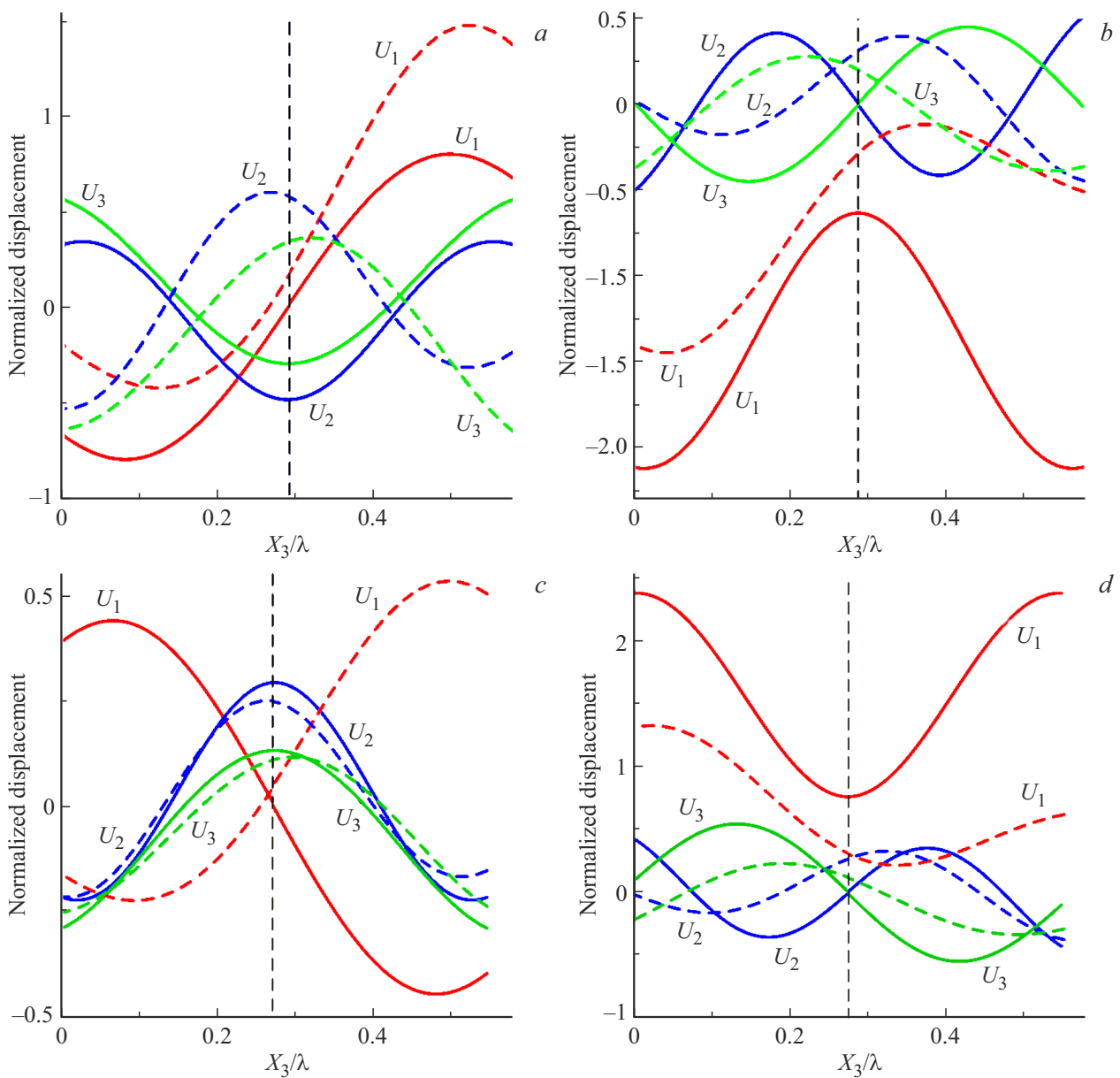


**Figure 3.** Normalized components of vector of elastic wave offset at  $h \times f = 6050$  m/s in Z-cut of crystal YBO and at  $h \times f = 5350$  m/s in Z-cut of crystal HBO at metallization of one and two free surfaces of wafer of crystal YBO. a) mode  $A_1$  YBO; b) mode  $SH_2$  YBO; c) mode  $A_1$  HBO; d) mode  $SH_2$  HBO.

of 5150 m/s to 6750 m/EMCC changes from 0.002 to 0.007 for mode  $A_1$  and from 0.005 to 0.01 for mode  $SH_2$ . Similar hybridization exists in wafer of crystal YBO between modes  $S_2$  and  $SH_3$  in region  $h \times f$  near 9050 m/s. EMCC values change from 0.002 to 0.01 in wafer of crystal YBO. The occurrence of interaction of elastic wave modes during metallization of only one free surface in this case is caused by change in the elastic wave polarization. Figure 3 presents vectors of offset of interacting modes  $A_1$  and  $SH_2$ . Solid lines show the components of offset vector for free surface, but dashed lines at one metallized surface of crystal wafer.

At free or short circuited both free surfaces of wafer the components of offset vector of elastic wave are strictly

symmetrical relative to central plane equidistant from both surfaces of the wafer (Figure 3). In case of short circuited the surface the offset profiles of mode  $A_1$  and  $SH_2$  become asymmetric relative to central plane (Figure 3). In particular, offset of component  $U_1$  of offset vector of mode  $A_1$  of elastic wave is  $X_3/\lambda = 0.04$  from central plane, equidistant from both surfaces of the wafer of crystal YBO. For crystal HBO offsets of mode  $A_1$  of elastic wave are  $X_3/\lambda = 0.01$ . More significant change of values of component of offset vector occurs at one short circuited free surface. Due to similar changes of components of offset vectors of elastic wave there is interaction between modes of elastic waves, in particular between modes  $A_1$  and  $SH_2$  (Figure 3). Same

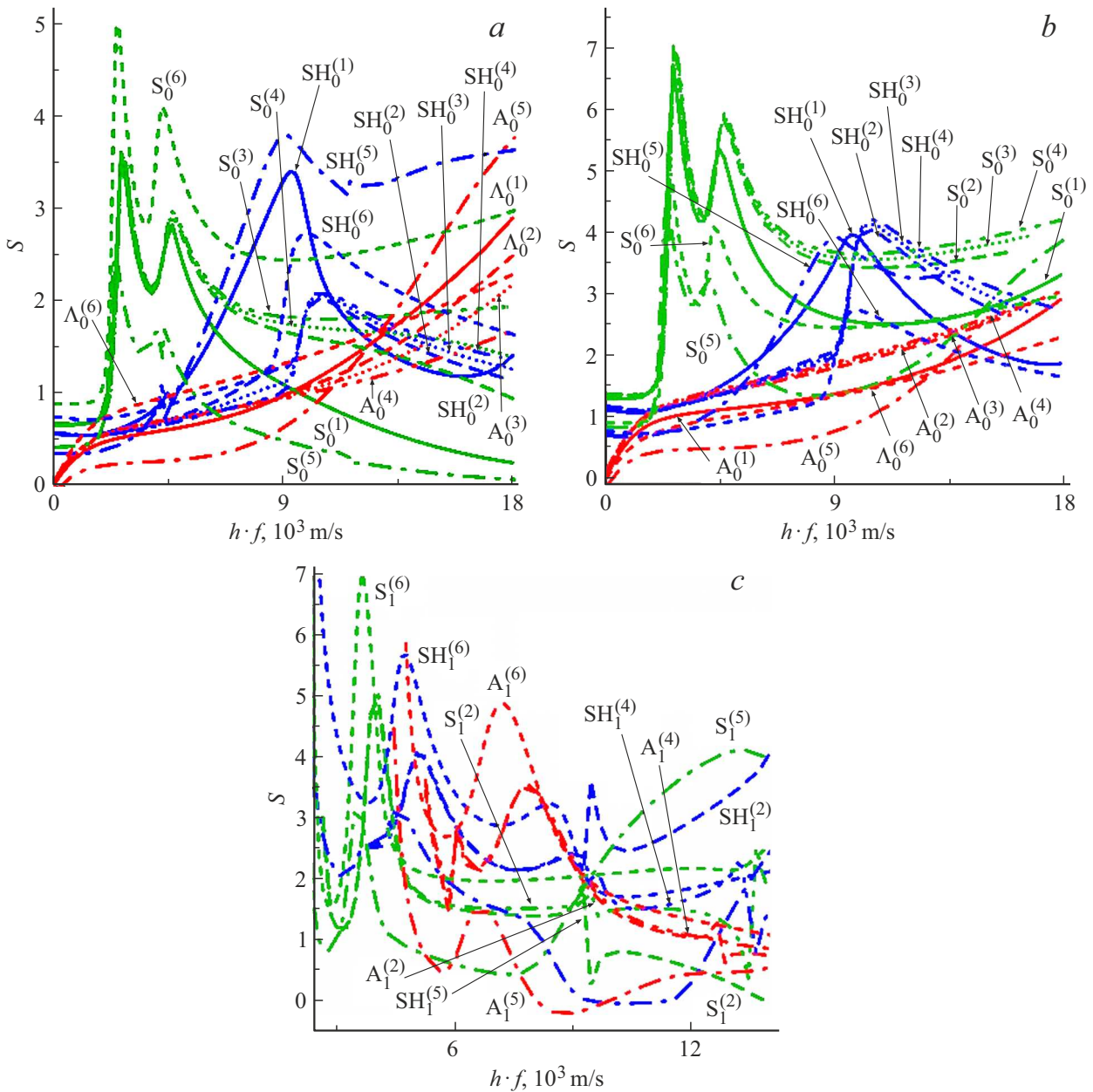


**Figure 4.** Dispersion dependence of mass sensitivity  $S$  for modes of Lamb wave from  $h \times f$ . *a, b*) fundamental modes  $A_0, S_0, SH_0$ ; *c*) mode  $A_1-SH_2$ . *a, c*) Al/YBO; Al/HBO *b*) Al/YBO/Al; Al/HBO/Al.

effect was described in [26], but for laminar structure depending on geometric asymmetry of multilayer structure and layer thickness.

Let's consider effect of mass load of metal layer on properties of Lamb waves. Important characteristic is normalized gravimetric (mass) sensitivity of the acoustic wave to mass load on surface of acoustic line, determined as [20,27]:

$$S = \frac{1}{d\rho_0} \left( \frac{\Delta V}{\Delta V_{met}} \right), \quad (4)$$

where  $\Delta V = V - V_{met}$  relative change of phase speed of SAW considering metal layer with density  $\rho_0$ .  $V_{met}$  —

phase speed of elastic wave upon deposition of thin metal layer not changing mechanical boundary conditions. The change in the phase speed modes of the elastic wave was calculated with relative ratios of thicknesses of the metal layers to thickness of the piezoelectric at  $d/h = 10^{-4}, 0.001, 0.01, 0.1$ , where  $d$  — thickness of metal layer and  $h$  — thickness of piezoelectric wafer. Figure 4 presents graphs of mass load  $S$  in laminar structures „Al/YBO“, „Al/YBO/Al“, „Al/HBO“ and „Al/HBO/Al“ depending on ratio  $d/h$  and parameter  $h \times f$ . For fundamental modes of Lamb wave  $A_0, S_0$  and  $SH_0$  waves in structures with metallization of one and both free surfaces the nature of behavior of coefficient  $S$  is qualitatively similar (Figure 4, *a, c*),

but numerical values  $S$  for the structure with two-side metallization of type „Al/YBO/Al“ practically by two times exceed appropriate values for structure with single-side metallization of type „Al/YBO“. Note that at values  $h \times f$  up to 6000 m/s the effect of thickness  $d$  of metal layer on change of coefficient  $S$  is insignificant. In graphs Figure 4,  $a, c$  changes of coefficient  $S$  practically does not differ for structures with piezoelectric YBO. For laminar structure based on piezoelectric HBO changes of numerical values of coefficient  $S$  are more significant, as density of crystal HBO exceeds density of crystal YBO.

But for modes of elastic wave of higher order the nature of behavior of mass load  $S$  significantly differs from structure of type „Al/YBO/Al“ (Figure 4,  $b$ ), this is due to interaction (hybridization) of modes of elastic wave in structure similar to „Al/YBO“. The thickness increasing of Al layer increases the hybridization effect, which causes sharp changes in the values of the coefficient  $S$  in the hybridization region. Note that value  $d/h$  increasing increases asymmetry and, accordingly, degree of hybridization of modes of elastic wave. Besides, upon value  $d/h$  increasing the values of coefficient  $S$  decrease for the symmetric mode  $S_0$ , but for the mode of elastic wave  $A_0$ ,  $SH_0$  values  $S$  on the contrary increase (Figure 4).

## 4. Conclusion

Studies of electromechanical characteristics of crystals with structure of oxyborates  $YAl_3(BO_3)_4$  and  $HoAl_3(BO_3)_4$  are performed. Full set of permanent material tensors of crystals is provided. Characteristics of elastic waves BAW, SAW, SH-waves and lamb waves in wafers of these single-crystals are studied. It is noted that although densities of crystals  $YAl_3(BO_3)_4$  and  $HoAl_3(BO_3)_4$  significantly differ, the acoustic characteristics of single-crystals are qualitatively same and differ insignificantly by value. The metallization of one free surface of crystal plane leads to symmetry of components of offset vector of elastic waves relative to central plane, equidistant from free surfaces of waver. This causes hybridization of modes of elastic wave. The mass load of the metal layer increasing leads to increase in the hybridization effect. Based on the obtained data we can conclude on future possible use of crystals YBO and HBO in devices of acoustic electronics. Especially considering that these crystals belong to the symmetry group 32, and in the future may have thermally stable directions of propagation of elastic waves, which is area for further study.

## Conflict of interest

The authors declare that they have no conflict of interest.

## References

- [1] D. Khomskii. *Physics*, **2**, 20, ??? (2009).
- [2] R. Ramesh, N.A. Spaldin. *Nature Mater.* **6**, 21 (2007).

- [3] N.A. Spaldin, M. Fiebig. *Science* **309**, 5733, 391 (2005).
- [4] K.C. Liang, R.P. Chaudhury, B. Lorenz, Y.Y. Sun, L.N. Bezmaternykh, V.L. Temerov, C.W. Chu. *Phys. Rev. B* **83**, 18, 180417 (2011).
- [5] A.A. Mukhina, G.P. Vorob'ev, V.Yu. Ivanov, A.M. Kadomtseva, A.S. Narizhnaya, A.M. Kuz'menko, Yu.F. Popov, L.I. Bezmaternykh, I.A. Gudim. *Pis'ma v ZhETF* **93**, 5, 305 (2011). (in Russian).
- [6] K.N. Gorbachenya, V.E. Kisel, A.S. Yasyukevich, N.V. Kuleshov, V.V. Maltsev, N.I. Leonyuk. *Pribory i metody izmerenij* **2**, 5, 79 (2012). (in Russian).
- [7] A.S. Aleksandrovsky, I.A. Gudim, A.S. Krylov, A.V. Malakhovskii, V.L. Temerov. *J. Alloys Compd.* **496**, 1–2, L18 (2010).
- [8] G. Wang, H.G. Gallagher, T.P.J. Han, B. Henderson. *Rad.Eff. Def. Sol* **136**, 1–4, 43 (1995).
- [9] L. Zheng, R. Jinlei, L. Pascal, A. Gerard, T. Takunori, R. Daniel. *CLEO: QELS Fundamental Science JTU5A*, 33 (2015).
- [10] N.V. Volkov, I.A. Gudim, E.V. Eremin, A.I. Begunov, A.A. Demidov, K.N. Boldyrev. *Pis'ma v ZhETF* **99**, 2, 72 (2014). (in Russian).
- [11] A.I. Popov, D.I. Plokhov, A.K. Zvezdin. *Phys. Rev. B* **87**, 2, 024413 (2013).
- [12] A.K. Zvezdin, S.S. Krotov, A.M. Kadomtseva, G.P. Vorobiev, Yu.F. Popov, A.P. Pyatakov, L.N. Bezmaternykh, E.N. Popova. *Pis'ma v ZhETF* **81**, 6, 335 (2005). (in Russian).
- [13] T.N. Gaydamak, I.A. Gudim, G.A. Zvyagina, I.V. Bilych, N.G. Burma, K.R. Zhekov, V.D. Fil. *FNT* **41**, 8, 792 (2015). (in Russian).
- [14] V.I. Zinenko, M.S. Pavlovskiy, A.S. Krylov, I.A. Gudim, E.V. Eremin, *ZhETF* **144**, 6, 1174 (2013). (in Russian).
- [15] G.A. Zvyagina, K.R. Zhekov, L.N. Bezmaternykh, I.A. Gudim, I.V. Bilych, A.A. Zvyagin. *FNT* **34**, 1, 1142 (2008). (in Russian).
- [16] P.P. Turchin, S.I. Burkov, V.I. Turchin, S.V. Yurkevich, P.O. Sukhodaev, I.S. Raikova. *J. Sib. Fed. Univ. — Math. Phys.* **12**, 6, 756 (2019).
- [17] P.P. Turchin, V.I. Turchin, S.V. Yurkevich, P.O. Sukhodaev, I.S. Raikova. *J. Sib. Fed. Univ. — Math. Phys.* **13**, 1, 97 (2020).
- [18] D. Royer, E. Dieulesaint. *Elastic waves in solids II: generation, acousto-optic interaction, applications.* SSBM. (1999). 446 p.
- [19] L.A. Victorov. *Rayleigh and Lamb waves.* Plenum Press. N. Y. (1967). 154 c.
- [20] S.I. Burkov, O.P. Zolotova, B.P. Sorokin, P.P. Turchin, V.S. Talismanov. *J. Acoust. Soc. Am.* **143**, 1, 16 (2018).
- [21] J. Rajagopalan, K. Balasubramaniam, C.V. Krishnamurthy. *J. Acoust. Soc. Am.* **119**, 2, 872 (2006).
- [22] K.S. Alexandrov, G.T. Prodayvoda. *Anizotropiya uprugikh svojstv mineralov i gornykh porod.* Izdatel'stvo SO RAN, Novosibirsk. (2000). 353 s. (in Russian).
- [23] J.F. Nye. *Physical properties of crystals: their representation by tensors and matrices.* OUP, (1985). 329 p.
- [24] P.P. Turchin, S.I. Burkov, V.I. Turchin, O.N. Pletnev, M.Yu. Chulkova, A.G. Nechepuryshina. *J. Sib. Fed. Univ. — Math. Phys.* **15**, 1, 80 (2022).
- [25] I.E. Kuznetsova, B.D. Zajtsev, A.A. Teplykh, I.A. Borodina. *Akust. zh.* **53**, 1, 73 (2007). (in Russian).
- [26] E. Verona, V.I. Anisimkin, V.A. Osipenko, N.V. Voronova. *Ultrasonics* **76**, 4, 227 (2017).
- [27] G. Wingqvist, V. Yantchev, I. Katardjiev. *Sensor Actuat. A: Phys* **148**, 1, 88 (2008).

Translated by I.Mazurov